DISULFIDE CONNECTIVITY PREDICTION WITH EXTREME LEARNING MACHINES

Monther Alhamdoosh, Castrense Savojardo, Piero Fariselli and Rita Casadio
Biocomputing Group, University of Bologna, Via Irnerio 42, 40127 Bologna, Italy

Keywords: Disulfide connectivity, Disulfide bonds, Extreme learning machine, Backpropagation, ELM outperforms BP, Multiple feature vectors, Disulfide proteins, Disulfide bridge prediction, K-mean clustering with ELM, RBF networks with ELM, SLFN with ELM.

Abstract: Our paper emphasizes the relevance of Extreme Learning Machine (ELM) in Bioinformatics applications by addressing the problem of predicting the disulfide connectivity from protein sequences. We test different activation functions of the hidden neurons and we show that for the task at hand the Radial Basis Functions are the best performing. We also show that the ELM approach performs better than the Back Propagation learning algorithm both in terms of generalization accuracy and running time. Moreover, we find that for the problem of the prediction of the disulfide connectivity it is possible to increase the predicting performance by initializing the Radial Basis Function kernels with a k-mean clustering algorithm.
Finally, the ELM procedure is not only very fast but the final predicting networks can achieve an accuracy of 0.51 and 0.45, per-bonds and per-pattern, respectively. Our ELM results are in line with the state of the art predictors addressing the same problem.

1 INTRODUCTION

The prediction of protein structures from their sequences is still an open problem in Structural Bioinformatics, especially considering that the disproportion between the huge number of putative protein sequences with respect to the smaller number of known 3D structures. Over the last two decades several approaches were described in order to find approximate solutions to the protein folding problem and tools have been developed to facilitate the search of a likely structural template for the protein sequence at hand. Among these, the identification of the correct pairing of bonded cysteines in the protein sequence (disulfide connectivity) helps in constraining its folded structure.

The problem of the prediction of disulfide connectivity can be logically split into two steps: 1) predicting the disulfide-bonding state (namely the identification of the cysteine residues that in the protein chain are/are not likely to make disulfide bonds); 2) assigning the connectivity pattern of the bonded cysteines. For the first step several methods are available and achieve an average per-protein accuracy higher than 80% (Muskal et al., 1990; Fiser et al., 1992; Fariselli et al., 1999; Fiser and Simon, 2000; Mucchielli-Giorgi et al., 2002; Martelli et al., 2002; Chen et al., 2004; Liu, 2007). Finding solutions for the second step is generally harder than for the first one, since cysteine pairing in the protein space is a problem of global optimization in the protein feature space and the bridge formation is not necessarily dependent on local functional and structural motifs. Machine learning and computational methods have been widely used to solve the disulfide connectivity prediction problem over the past years with significant progresses.

Fariselli and Casadio (2001) first addressed the prediction of disulfide connectivity as a combinatorial optimization problem that finds the maximum-weight perfect matching of a complete undirected weighted graph. According to this graph model vertices are the putative bonded cysteines and edges represent the strength of interactions among corresponding cysteine pairs. Since the graph is complete, the Edmond-Gabows (EG) algorithm (Gabow, 1975) is the most suitable method to solve the corresponding Linear Programming problem. The weight edges were computed using stochastic optimization methods (Fariselli and Casadio, 2001) or neural networks (Fariselli et al., 2002; Shi et al., 2008).

Later other methods were developed and these in-

Alhamdoosh M., Savojardo C., Fariselli P. and Casadio R..
DISULFIDE CONNECTIVITY PREDICTION WITH EXTREME LEARNING MACHINES.
DOI: 10.5220/0003125600050014
In *Proceedings of the International Conference on Bioinformatics Models, Methods and Algorithms* (BIOINFORMATICS-2011), pages 5-14
ISBN: 978-989-8425-36-2

clude a bi-recursive neural network system (Vullo and Frasconi, 2004), a method based on Cysteine Separation Profiles (CSPs) (Zhao et al., 2005), neural networks that exploit diresidue composition (Ferrè and Clote, 2005), two dimensional recursive neural networks (Baldi et al., 2005), K-nearest neighbors algorithm (Chen et al., 2006), support vector regression (Song et al., 2007; Zhu et al., 2010), support vector machines (Lu et al., 2007), statistical analysis including correlated mutations (Rubinstein and Fiser, 2008), decomposition convolution kernels (Vincent et al., 2008) and recently prediction based on comparative modeling (Lin and Tseng, 2010).

Although it is difficult to compare the performance of different predictors, often trained and tested on different protein sets with different levels of homology, and implementing different protein features, the present best performance is in the range of 50-60% per protein accuracy depending on the number of disulfide bridges. In any case all the above approaches are poorly performing when the number of bridges in the protein is ≥ 5. This was/and still remains due to the paucity of examples in the PDB database of proteins with a large number (≥ 5) of disulfide bridges included in the training/testing set. In most of the neural network based methods quoted above the networks were modeled as directed acyclic graphs (DAG) trained with the very popular back-propagation (BP) algorithm that implements the steepest gradient descent (GD) search through the space of network weights. Trapping in local minima is one of the major problem of this procedure and the search in the weights space is generally slow and time-consuming, especially considering that the number of training examples in the biological data bases is exponentially increasing and methods need learning updating.

In this paper, we are approaching the problem of disulfide connectivity prediction using single-hidden layer feed-forward neural network (SLFN), with a latest machine learning technology called the Extreme Learning Machine (ELM) (Huang et al., 2004). We investigate the performance of this algorithm with different activation functions as compared to the classical BP approach. We find that the ELM procedure is very fast and that the final predicting networks can achieve an accuracy of 0.51 and 0.45, per-bonds and per-pattern respectively. Our ELM results are therefore in line with the state of the art predictors addressing the same problem and are obtained with less computational time.

The remainder of the paper is organized as follows: Section 2 describes the ELM learning algorithm. Section 3 presents our dataset and the experimental protocol of our work. Section 4 shows and discusses results, and concludes this paper.

2 BRIEF OF THE EXTREME LEARNING MACHINE

Single-hidden layer feed-forward neural network (SLFN) have been showed to be sufficient to solve very difficult mapping (Huang, 2003; Tamura and Tateishi, 1997). However, traditional learning algorithms for feed-forward networks, like back-propagation, require tuning many parameters over an iterative procedure that is very time-consuming. To overcome this issue, in the recent years the Extreme Learning Machines have been introduced (Huang et al., 2006b; Huang et al., 2004; Huang and Siew, 2004; Huang and Siew, 2005; Huang et al., 2006a). For sake of clarity we briefly introduce the mathematical notation used to define ELM.

2.1 Mathematical Perspective on SLFNs

For N arbitrary distinct samples (x_i, t_i), where $x_i = [x_{i1}, x_{i2}, \cdots, x_{in}]^T \in R^n$ and $t_i = [t_{i1}, t_{i2}, \cdots, t_{im}]^T \in R^m$, a standard SLFN with N hidden neurons and an activation function $g(x)$ is mathematically modeled as

$$\sum_{i=1}^{\tilde{N}} \beta_i g(w_i.x_j + b_i) = o_j, j = 1, \cdots, N \qquad (1)$$

where $w_i = [w_{i1}, w_{i2}, \cdots, w_{in}]^T$ is the weight vector connecting the ith hidden neuron and the input neurons, $\beta_i = [\beta_{i1}, \beta_{i2}, \cdots, \beta_{im}]^T$ is the weight vector connecting the ith hidden neuron and the output neurons, and b_i is the threshold of the ith hidden neuron. $w_i \cdot x_j$ denotes the inner product of w_i and x_j. The standard SLFNs can approximate these N samples with zero error if there exist β_i, w_i and b_i such that

$$\sum_{i=1}^{\tilde{N}} \beta_i g(w_i.x_j + b_i) = t_j, j = 1, \cdots, N \qquad (2)$$

The above N equations can be written compactly as:

$$H\beta = T \qquad (3)$$

where

$$H(w_1, \cdots, w_N, b_1, \cdots, b_N, x_1, \cdots, x_N) = \begin{bmatrix} g(w_1.x_1 + b_1) & \cdots & g(w_{\tilde{N}}.x_1 + b_{\tilde{N}}) \\ \vdots & \cdots & \vdots \\ g(w_1.x_N + b_1) & \cdots & g(w_{\tilde{N}}.x_N + b_{\tilde{N}}) \end{bmatrix}_{N \times \tilde{N}} \qquad (4)$$

$$\beta = \begin{bmatrix} \beta_1^T \\ \vdots \\ \beta_{\tilde{N}}^N \end{bmatrix}_{\tilde{N}\times m} \quad and \quad T = \begin{bmatrix} t_1^T \\ \vdots \\ t_{\tilde{N}}^N \end{bmatrix}_{\tilde{N}\times m} \qquad (5)$$

H is called the hidden layer output matrix of the neural network (Huang, 2003); the ith column of H is the ith hidden neuron output with respect to inputs $x_1, x_2, \dots, x_N$.

The same formulation can be extended to Radial Basis Function (RBF) networks, where each $g(w_i.x_i + b_i)$ in the hidden layer matrix H is substituted with a RBF kernel:

$$\phi_i(x) = \phi\left(\frac{\|x-\mu_i\|}{\sigma_i}\right) \qquad (6)$$

where $\mu_i = [\mu_{i1}, \mu_{i2}, \dots, \mu_{in}]^T$ is the ith kernelś center and σ_i is its impact width.

2.2 ELM Learning Algorithm

Since the number of distinct training examples is usually much greater than the number of hidden neurons ($N \gg \tilde{N}$), the H matrix is a rectangular matrix and tuning the parameters w_i, b_i, β_i or $\mu_i, \sigma_i, \beta_i (i = 1, \dots, \tilde{N})$ in order to obtain a unique solution for $H\beta = T$ is not always possible. Gradient–based learning algorithms try to find a solution that minimizes the cost function

$$E = \sum_{j=1}^{N}\left(\sum_{i=1}^{\tilde{N}} \beta_i f_i(x_j) - t_j\right)^2 \qquad (7)$$

where $f_i(x_j)$ is the output of the ith hidden neuron (additive or RBF kernel) when the training sample x_j is introduced to the network.

Seeking simplicity, Huang et al. (Huang et al., 2004; Huang and Siew, 2004; Huang and Siew, 2005; Huang et al., 2006a) showed that there is no need to tune the input weights and biases of hidden neurons or of the kernel parameters and that they can be randomly set and then fixed. Assuming the input weights and biases or kernel parameters are fixed, the training of SLFN is simply finding a solution $\hat{\beta}$ for the linear system $H\beta = T$. Usually this is achieved by adopting the Moor-Penrose generalized inverse (see theorem in P.147 of (Serre, 2002)), as:

$$\hat{\beta} = H^{\dagger}T \qquad (8)$$

where $H^{\dagger}$ is the pseudoinverse matrix of the hidden layer output matrix H. As analyzed by Huang et al., this method can reach good generalization performance by ensuring two properties of learning: the smallest norm of weights besides the smallest squared error on the training samples, while the gradient-based algorithms focuses on the later property only. The three main steps involved in ELM algorithm can be summarized as:

ELM Algorithm (Huang et al., 2004; Huang and Siew, 2004)**.** Given a training set $D = \{(x_i, t_i) | x_i \in R^n, t^i \in R^m, i = 1, \dots, N\}$, activation function g or kernel function ϕ, and number of hidden neurons or kernels $\tilde{N}$,
Step 1 Assign randomly input weights w_i and biases b_i for additive neurons or centers μ_i and impact widths $\sigma_i, i = 1, \dots, \tilde{N}$ for RBF kernels.
Step 2 Calculate the hidden layer output matrix H.
Step 3 Calculate the output weights β: $\hat{\beta} = H^{\dagger}T$.

The efficiency of this algorithm comes from its ability to use many nonlinear activation and kernel functions without restriction for being differential, and to avoid the troubling issues such as stopping criteria, learning rate, learning epochs and local minima.

3 IMPLEMENTATION AND METHODS

3.1 Dataset PDB0909

From the Protein Data Bank (PDB) (Berman et al., 2000), release of September 2009 we retrieved all protein structures that are resolved by X-ray experiments with resolution between 0 and 2.5 A°. Similar sequences were removed at 70% identity, then the chain with longest length and highest resolution for each protein was selected. To eliminate the redundancy we followed this procedure: an all-against-all BLAST (Altschul et al., 1990) sequence search was performed on the starting protein set, then we clustered similar chains together (as connected components of an undirected graph) and only the longest chain of each cluster was retained as representative. Two protein chains are defined similar if they share a sequence identity $> 25\%$ and an alignment coverage $> 80\%$. After this basic filtering process, we sorted out only the protein chains that have at least two intra-chain bonded cysteines, so that we ended up with 796 chains. In our study, we only focus on the chains that have 2, 3, 4, and 5 intra-chain disulfide bonds since chains with more than 5 bridges are very few and cannot be statistically tested (chains with one disulfide bridge are trivial cases). Table 1 shows the number of chains with 2, 3, 4 and 5 bridges and other statistics about each connectivity size. The % Coverage of Patterns Space column shows the lack of patterns representation when the number of bonded cysteines gets higher than eight.

3.2 Cross-validation Sets

A 4-fold cross-validation procedure was used to evaluate the performance of our predictor, in which the dataset is partitioned into four almost-equal-size subsets. The results obtained for the four tests are combined to produce a single evaluation. In order to guarantee the absence of homology among the folds we further re-aligned with BLAST all the sequences against themselves. We then defined two sequences as similar if their identity is $> 25\%$. According to this labeling, similar sequences were then clustered and chains of the same cluster were assigned to the same cross-validation fold.

3.3 Measures of Performance

Given a protein primary sequence with $N(=2B)$ cysteines forming B disulfide bridges, the number of possible cysteine pairs is:

$$N_c = \binom{2B}{2} = \frac{2B!}{2!(2B-2)!} = B(2B-1), \qquad (9)$$

and the number of possible connectivity patterns is:

$$N_p = (2B-1)!! = \frac{(2n)!}{2_n.n!} \qquad (10)$$

The number of possible connectivity patterns dramatically grows as the number of disulfide bridges increases. For this reason among the several indexes that can be used to score the predictions (Ferrè and Clote, 2005; Baldi et al., 2005), the most informative are: the disulfide bond index Q_c and disulfide pattern index Q_p (Fariselli and Casadio, 2001). Q_p, globally evaluates the ability of a predictive system to correctly predict disulfide connectivity patterns and is given by:

$$Q_p = \frac{\sum_{i=1}^{T_p} \delta_i(x,y)}{T_p}, \qquad (11)$$

where $\delta_i(x,y)$ is equal to 1 if the predicted pattern y of the ith protein coincides with its correct pattern x and T_p is the total number of predicted protein chains. In 4-fold cross-validation, we collect the numbers of correctly predicted patterns from all folds, and then average them over the size of the un-partitioned dataset. Alternatively, Q_c is a pair-wise index that estimates the predictive accuracy of individual disulfide bonds i.e. the percentage of disulfide bridges that are correctly predicted, and is given by:

$$Q_c = \frac{\sum_{i=1}^{T_p} \sum_{j=1}^{B} \delta_j(x,y)}{T_c}, \qquad (12)$$

where $\delta_j(x,y)$ is equal to 1 if the jth predicted disulfide bond y of the ith predicted pattern coincides with a correct disulfide bond x in the correct pattern, B is the connectivity size of the ith pattern, and T_c is the total number of possible pairs in the T_p proteins. Similarly, the numbers of correctly predicted pairs are collected from all folds during cross-validation and the total Q_c value is computed by averaging these numbers over the total number of pairs in the un-partitioned dataset.

To score the performance we define a *random predictor* R_p without bias a predictor that assigns randomly the bonding pairs. For R_p the performances can be theoretically computed as:

$$Q_p(R_p) = \frac{1}{N_p} = \frac{1}{(2B-1)!!} \qquad (13)$$

$$Q_c(R_p) = \frac{B}{N_c} = \frac{B}{B(2B-1)} = \frac{1}{2B-1} \qquad (14)$$

$Q_p(R_p)$ is vanishing much faster than $Q_c(R_p)$ although both depend on the number of disulfide bridges.

3.4 Multiple Feature Vectors

To assign pairwise probabilities we defined vectors that represent each cysteine pairs and some global protein descriptors (Song et al., 2007).

Local Descriptors

Evolutionary information: this descriptor constitutes the largest portion of our multiple sequence feature vectors that it is composed of $w*20*2$ components when the neighbor amino acidic residues around the two cysteine forming disufide bond are comprised in a window of size w. We evaluate different window sizes of the cysteine local context and found out that $w=13$ (six residues flanking the cysteine at each side) is the most appropriate value. Each position in the neighbor environment of cysteines, including the cysteine position, is encoded with 20 values that are the frequencies of each residue at this particular position. This evolutionary information is obtained using the PSI-BLAST program (Altschul et al., 1997) from the multiple sequence alignment portrayed in the form of position-specific scoring matrices (PSSM). The PSI-BLAST was run against the non-redundant database for 3 iterations with an E-value cutoff of 0.001.

Secondary Structure Information: it is also a key player in improving the prediction accuracy increasing the training vectors with new informative attributes relative to the local environment of cysteines. In this paper, the DSSP program (Kabsch and Sander,

Table 1: The PDB0909 Dataset. % Coverage of Patterns Space represents the percentage of disulfide patterns, out of all possible patterns, that are observed in our dataset. e.g. for B=2, the patterns space contains 3 patterns (C1C2, C3C4), (C1C3, C2C4), (C1C4, C2C3). % Coverage of Pairs Space represents the same value, but in terms of ordered cysteine pairs. e.g. for B=2, the pairs space is composed of 6 pairs (C1C2, C1C3, C1C4, C2C3, C2C4, C3C4).

Connectivity Size (B)	# of Chains	# of Bonded Cysteines	# of Free Cysteines	Total # of Cysteines	% Coverage of Patterns Space	% Coverage of Pairs Space
2	146	584	103	687	100	100
3	104	624	60	684	100	100
4	52	416	20	436	25.71	100
5	40	400	17	417	3.39	84.44
Total	342	2024	200	2224	7.21	92.55

1983) was used to obtain the secondary structure information which was encoded into a 3-letters representation. The letter *A* represents the alpha helix (H), 3-helix (G) and 5 helix (I) from the DSSP output, the letter *B* encodes for the residues in isolated bridges (B) and extended strands (E) in the DSSP output, and finally the letter *C* stands for the hydrogen bonded turns (T), the bends (S) and the loops and irregular elements (blank). Technically, each letter was encoded by three binary bits: 100 for A, 010 for B, 001 for C and 000 for X (*empty place*). This descriptor contributes 39 components $(13*3)$ for each training vector when $w = 13$.

Global Descriptors

Residues Composition: it describes the residues content in a protein sequence as 20-dimensions vector of the relative frequencies of residues of different types. These dimensions can be mathematically formulated as following:

$$AA_i = \frac{n_i}{L}; i = 1, \ldots, 20 \tag{15}$$

where n_i is the number of occurrences of the residues of type i in the sequence and L is the length of the protein sequence.

Protein Sequence Length: when considering a protein i with $\acute{L}_i$ residues from a proteins dataset, the normalized protein length L_i is given by:

$$L_i = \frac{\acute{L}_i - \bar{L}}{SD} \tag{16}$$

where the mean protein length $\bar{L}$ and the standard deviation SD of protein lengths are computed on the whole dataset.

Protein Molecular Weight: similarly to the equation above, for a protein i with M_i total molecular weight we normalized the value as:

$$M_i = \frac{\acute{M}_i - \bar{M}}{SD} \tag{17}$$

where the mean molecular weight $\bar{M}$ and the standard deviation SD are computed on the whole dataset. The molecular weight values for the single residues are taken from ProtScale (Gasteiger et al., 2005).

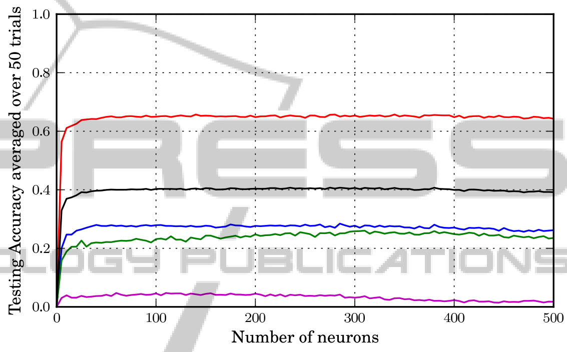

Figure 1: The testing accuracy of prediction when using additive neurons and training different connectivity sizes together. The red, blue, green and magenta curves represent the accuracies for 2, 3, 4 and 5 connectivty sizes, repsectively. The black curve represents the overall accuracy regardless of the connectivity size.

Cysteines Separation Distance: we coded the cysteine sequence separation as:

$$SEP(C_i, C_j) = log(|j - i|) \tag{18}$$

where i and j are the sequence positions of cysteines C_i and C_j, respectively.

Relative Order of Cysteines: this feature encodes for two different values of the input vector, representing the normalized relative order of the two cysteines. For instance, given a protein P with 4 cysteines (C_1, C_2, C_3, C_4) the corresponding normalized ordered list of cysteine is $(1/4, 2/4, 3/4, 4/4) = (0.25, 0.5, 0.75, 1)$. So that when the method train/predict a pair of cysteines the two corresponding values are taken from the list (e.g. the pair $[C_2, C_3]$ is encoded as $[0.5, 0.75]$).
As a result, the final training/testing vectors consist of 623 components based on these protein sequence features.

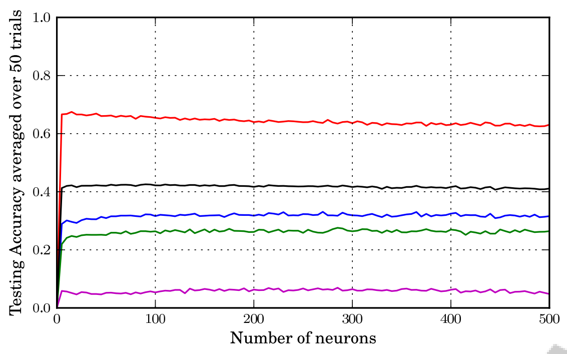

Figure 2: The testing accuracy of prediction when using L1 RBF kernels and training different connectivity sizes together.

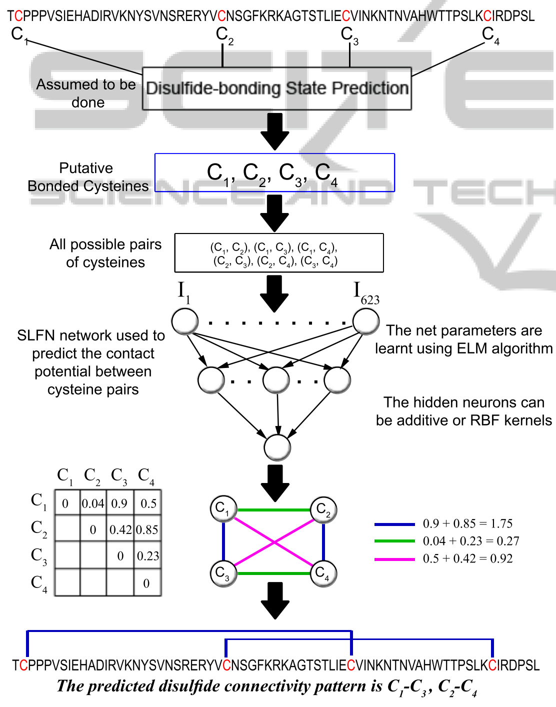
TCPPPVSIEHADIRVKNYSVNSRERYVCNSGFKRKAGTSTLIECVINKNTNVAHWTTPSLKCIRDPSL
C_1
C_2
C_3
C_4
Assumed to be done
Disulfide-bonding State Prediction
Putative Bonded Cysteines
C_1, C_2, C_3, C_4
All possible pairs of cysteines
$(C_1, C_2), (C_1, C_3), (C_1, C_4), (C_2, C_3), (C_2, C_4), (C_3, C_4)$
I_1
I_{623}
SLFN network used to predict the contact potential between cysteine pairs
The net parameters are learnt using ELM algorithm
The hidden neurons can be additive or RBF kernels
C_1 C_2 C_3 C_4
C_1 0 0.04 0.9 0.5
C_2 0 0.42 0.85
C_3 0 0.23
C_4 0
0.9 + 0.85 = 1.75
0.04 + 0.23 = 0.27
0.5 + 0.42 = 0.92
TCPPPVSIEHADIRVKNYSVNSRERYVCNSGFKRKAGTSTLIECVINKNTNVAHWTTPSLKCIRDPSL
The predicted disulfide connectivity pattern is C_1-C_3, C_2-C_4

Figure 3: The general scheme of our proposed disulfide connectivity prediction method. The steps of our procedure have been illustrated for the chain F of Interleukin-15 receptor protein whose PDB ID 2PSM.

3.5 Experimental Protocol

The implementation of the proposed model (see Figure 3) was done using the free scripting language Python 2.6 (Van Rossum et al., 1991) along with its numerical package Numpy 1.3 (Oliphant, 2006), used to compute the pseudo-inverse matrix of the matrix H in the ELM learning algorithm. Single experiment with different numbers of additive and kernel hidden neurons have been carried out to find the best estimation of the hidden layers size. Since some of the network parameters are randomly initialized, each experiment was run 50 times and then the average measurements were taken to evaluate the performance of our Model. The additive neurons were activated using the sigmoid activation function $g(x) = \frac{1}{1+e^{-x}}$ while two Gaussian functions $L_1(x) = e^{\frac{-\|x-\mu\|}{\sigma}}$ and $L_2(x) = e^{\frac{-\|x-\mu\|^2}{\sigma^2}}$ were tested for the RBF kernels. Furthermore, one output neuron was used in most of the experiments unless otherwise mentioned. We also examined the performance of the Backpropagation (BP) learning algorithm on SLFNs with a symmetric sigmoid activation function for the hidden layer and a sigmoid activation function for the output layer. The learning rate was set to 0.1 and MSE threshold error to 0.0001. Interestingly, early stopping condition based on the accuracy of validation sets has been also employed to avoid overfitting of training data and reduce training time. The online incremental approach was used to update weights.

The simulations were executed on a computer of 8 processors, each one with 2.5 GHz frequency, and 16 GB of RAM.

4 RESULTS AND DISCUSSION

We first evaluate the SLFN performance as a function of the number of hidden units adopting a four-fold cross validation procedure. The results at increasing number of additive neurons are reported in Figure 1 for the disulfide pattern index Qp. Similar graphs reporting the Qp values are shown in Figures 2 and 4 when the transfer function during the learning phase is the Gaussian function with L1 and L2 norms. In all reported cases, the SLFN performance reaches a plateau when the number of hidden neuron is larger than 100. It is worth noticing that the training time is nearly a linear function of the number of hidden neurons irrespectively of the transfer function adopted (Figure 5). The accuracy index Qp when plotted as a function of the number of hidden units obtained with the Back Propagation (BP) learning algorithm is less stable then that obtained with the EML learning (compare Fig.1,2,4 with Figure 6). Furthermore, the BP training time as a function of the number of hidden neurons shows a significantly steeper slope with respect to the ELM approach (compare Figures 5(a) and 5(b) with Figure 7). These results highlight the effective time saving of ELM with respect to BP when training is performed. The detailed results for the best performing number of neurons for the different SLFN models are reported in Table 2, where it is listed that the RBF networks with L1 function achieve the best overall performance both in term of Qc and Qp . This picture holds also when the performance is evaluated separately for each subset comprising proteins with a different number of disulfide bonds (Table 2). Table 2 reports also the required learning time, and it appears that the Back Propagation (BP) algorithm is far slower than the ELM algorithm.

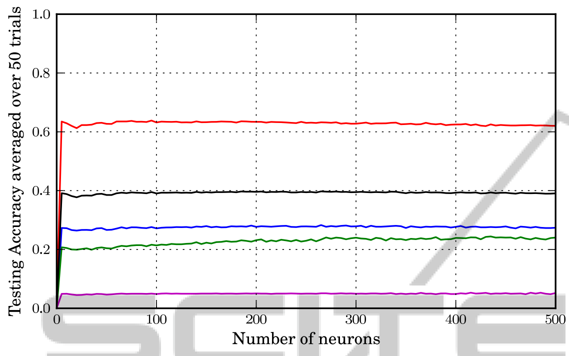

Figure 4: The testing accuracy of prediction when using L2 RBF kernels and training different connectivity sizes together.

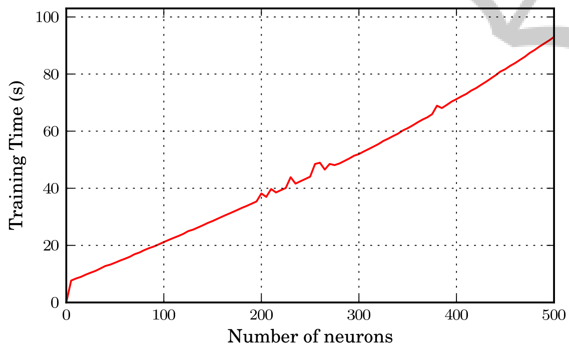

(a) Additive hidden neurons.

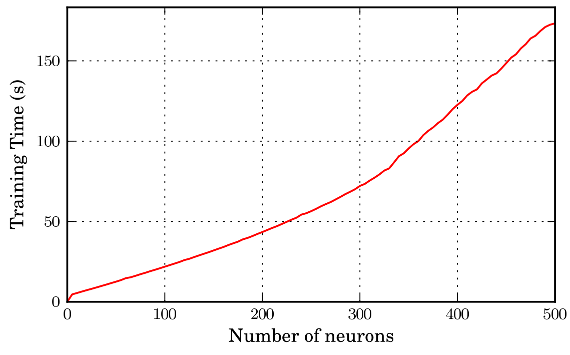

(b) RBF hidden neurons.

Figure 5: The training time of SLFNs over 4-folds cross-validation procedure when training different connectivity sizes together.

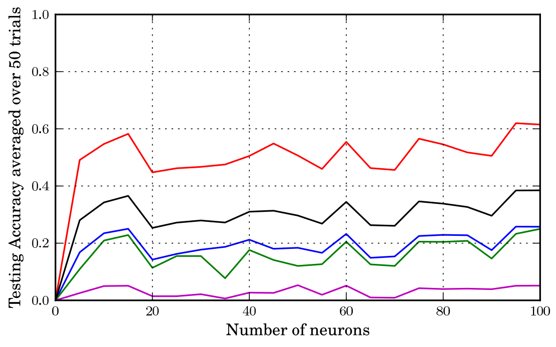

Figure 6: The testing accuracy of prediction when using BP learning algorithm and training different connectivity sizes together.

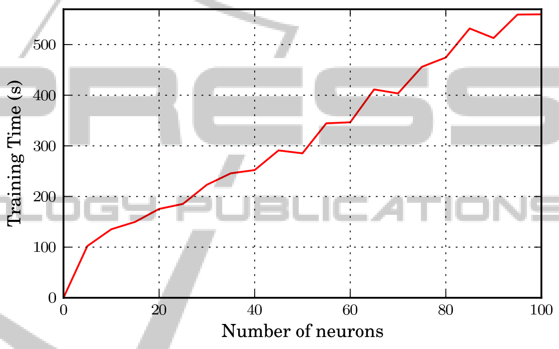

Figure 7: The training time of SLFNs over 4-folds cross-validation procedure when using BP learning algorithm and training different connectivity sizes together.

4.1 Performance Enhancement

Instead of random initializing the first layers of weights, we select them using a standard K-mean clustering approach to set the centers and impact widths of kernels. The value of the selected number of clusters K corresponds to the number of hidden neurons. Next, for each hidden kernel its center is set by the center of a cluster while its impact width is set as the standard deviation of the cluster vectors from its center. The performance of ELM with L1 Gaussian functions and K-mean clustering algorithm is reported in Figure 8 for Qp. The training time is dominated by the K-mean clustering procedure and can be several times greater than the random initialization (compare Figure 9 with Figure 5). This is particular evident by considering that the K-mean clustering running time increases with the number of clusters (K) up to a given threshold that depends on the ratio between the number of data and the K value.

Then the training time as a function of the number of hidden neurons decreases (Figure 9), becoming constant when K equates the number of elements to cluster. Nonetheless, the best results obtained by

Table 2: Comparison of different ELM-trained models with BP-trained model when different connectivity sizes are trained together. N_H is the best number of hidden neurons (when additive) and kernels (when RBF). Qc and Qp (%) have been thoroughly explained earlier. ELM (Sig) is a neural network trained with ELM algorithm using sigmoid activation function for the hidden neurons. ELM (L_i_RBF) is an RBF neural network trained with ELM algorithm using L_i Gaussian function. Time (s) is the average training time, given in seconds, of 50 experiments.

Model	B = 2		B = 3		B = 4		B = 5		Overall		Best # of	Time
	Q_c	Q_p	Q_c	Q_p	Q_c	Q_p	Q_c	Q_p	Q_c	Q_p	neurons	(s)
ELM (Sig)	65	65	42	28	42	24	27	4	46	41	150	28.52
ELM (L_1_RBF)	66	66	45	32	45	26	31	5	48	43	90	18.55
ELM (L_2_RBF)	64	64	42	28	39	22	28	5	45	40	95	18.55
BP	62	62	38	26	40	23	29	5	44	38	95	559.29

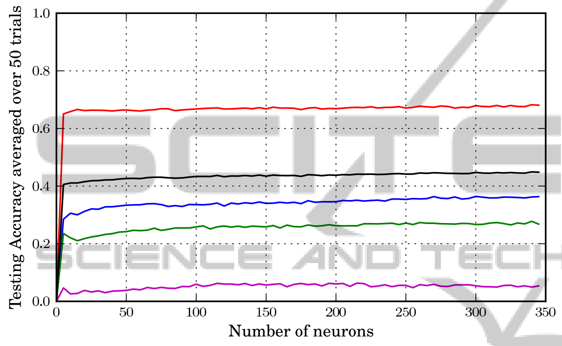

Figure 8: The testing accuracy of prediction when using K-Mean clustering algorithm to initialize L1 RBF kernels and training different connectivity sizes togehther.

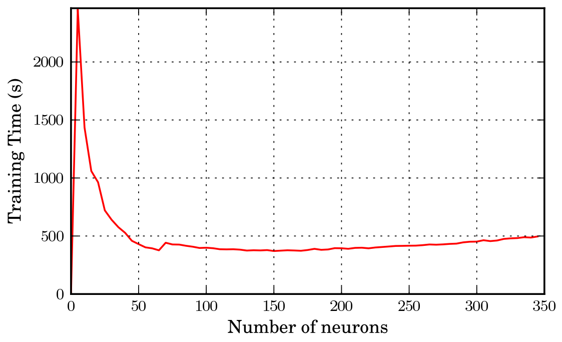

Figure 9: The training time of SLFNs over 4-folds cross-validation procedure when using K-mean clustering algorithm to initialize RBF kernels and training different connectivity sizes together.

using the K-mean clustering initialization are slightly better than the random initialization approach (Table 3).

4.2 Comparison with some Previous Works

As mentioned in the introduction it is not easy to compare our results with those obtained before, since different authors adopted different datasets (sometimes without reducing the sequence identity between training and testing sets). Nonetheless for sake of clarity in Table 4 we compare our best ELM cross-validation performance with the Random predictor R_p, the historical benchmark Fariselli et al. 2002, and two state of the art methods Vullo and Frasconi (2004) and Baldi et al. (2005). It is evident that all the methods perform better than the random predictor and that the ELM approach compare very well with the state of the art methods making it a fast and efficient alternative when the problem of the prediction of the disulfide connectivity is addressed.

Table 3: Our method performance with L1 RBF kernels initialized using k-mean clustering. The best number of hidden neurons is 270 and the corresponding training time is 425.11 seconds.

Connectivity Size	2	3	4	5	overall
Q_c	67	48	44	37	51
Q_p	67	36	27	6	45

5 CONCLUSIONS

In this paper we address the problem of the prediction of the disulfide connectivity using an Extreme Learning Machine approach. We test different activation functions of the hidden neurons and different way of initializing the first layer of weights. We also evaluate the performance of the different methods both in term of accuracy and running times. We show that the ELM learning is faster and generalizes better than the corresponding Back Propagation training. Among our tested models we verify that the RBF neural networks trained with an ELM procedure are the best performing approach for the task at hands. We find that a K-mean clustering procedure to select the first layer of weights, improves the overall EML accuracy

Table 4: Comparison with previous works on disulfide connectivity prediction. These results were generated on a benchmark dataset called SP39 (Fariselli and Casadio, 2001).

Proposed Method	B = 2		B = 3		B = 4		B = 5		Overall	
	Q_c	Q_p	Q_c	Q_p	Q_c	Q_p	Q_c	Q_p	Q_c	Q_p
R_p	33	33	20	7	14	1	11	0	19	10
Fariselli et al. (2002)	68	68	37	22	37	20	26	2	42	34
Vullo and Frasconi. (2004)	73	73	51	41	37	24	30	13	49	44
Baldi et al. (2005)	74	74	61	51	44	27	41	11	56	49
ELM	72	72	45	33	49	31	44	22	52	45

and that the trained neural system well compares with the state of the art methods.

ACKNOWLEDGEMENTS

The authors would like to acknowledge Dr. Dianhui Wang, from the Department of Computer Science and Computer Engineering at La Trobe University in Australia, for his valuable suggestions to utilize ELMs for the problem at hand.

REFERENCES

Altschul, S. F., Gish, W., Miller, W., Myers, E. W., and Lipman, D. J. (1990). Basic local alignment search tool. *Journal of Molecular Biology*, pages 403–410.

Altschul, S. F., Madden, T. L., Schaffer, A. A., Zhang, J., Zhang, Z., Miller, W., and Lipman, D. J. (1997). Gapped blast and psi-blast: a new generation of protein database search programs. *Nucleic Acids Research*, 25(17):3389–3402.

Baldi, P., Cheng, J., and Vullo, A. (2005). Large-scale prediction of disulphide bond connectivity. In Saul, L., Weiss, Y., and Bottou, L., editors, *Advances in Neural Information Processing Systems*, 17, pages 97–104. MA MIT Press.

Berman, H. M., Westbrook, J., Feng, Z., Gilliland, G., Bhat, T. N., Weissig, H., Shindyalov, L. N., and Bourne, P. E. (2000). The protein data bank. *Nucleic Acids Research*, 28(1).

Chen, G., Deng, H., Gui, Y., Pan, Y., and Wang, X. (2006). Cysteine separations profiles on protein secondary structure infer disulfide connectivity. In *IEEE International Conference on Granular Computing*.

Chen, Y., Lin, Y.-S., Lin, C.-J., and Hwang, J.-K. (2004). Prediction of the bonding states of cysteines using the support vector machines based on multiple feature vectors and cysteine state sequences. *Proteins*, 55:1036–1042.

Fariselli, P. and Casadio, R. (2001). Prediction of disulfide connectivity in proteins. *Bioinformatics*, 17(10):957–964.

Fariselli, P., Martelli, P. L., and Casadio, R. (2002). A neural network-based method for predicting the disulfide connectivity in proteins. In Damiani, E., editor, *Knowledge Based Intelligent Information Engineering Systems and Allied Technologies (KES)*, pages 464–468. Amsterdam IOS Press.

Fariselli, P., Riccobelli, P., and Casadio, R. (1999). Role of evolutionary information in predicting the disulfide-bonding state of cysteine in proteins. *Proteins*, 36:340–346.

Ferrè, F. and Clote, P. (2005). Disulfide connectivity prediction using secondary structure information and diresidue frequencies. *Bioinformatics*, 21(10):2336–2346.

Fiser, A., Cserzo, M., Tudos, E., and Simon, I. (1992). Different sequence environments of cysteines and half cystines in proteins: Application to predict disulfide forming residues. *FEBS*, 302(2):117–120.

Fiser, A. and Simon, I. (2000). Predicting the oxidation state of cysteines by multiple sequence alignment. *Bioinformatics*, 16(3):251–256.

Gabow, H. N. (1975). An efficient implementation of edmonds al- gorithm for maximum weight matching on graphs. Technical Report CU-CS-075-75, Department of Computer Science, Colorado University.

Gasteiger, E., Hoogland, C., Gattiker, A., Duvaud, S., Wilkins, M. R., Appel, R. D., and Bairoch, A. (2005). Protein identification and analysis tools on the expasy server. In Walker, J. M., editor, *The Proteomics Protocols Handbook*, pages 571–607. Humana Press.

Huang, G.-B. (2003). Learning capability and storage capacity of two-hidden-layer feedforward networks. *IEEE Transaction on Neural Networks*, 14(2).

Huang, G.-B. and Siew, C.-K. (2004). Extreme learning machine: Rbf network case. In *he Proceedings of the Eighth International Conference on Control, Automation, Robotics and Vision (ICARCV)*.

Huang, G.-B. and Siew, C.-K. (2005). Extreme learning machine with randomly assigned rbf kernels. *International Journal of Information Technology*, 11(1):16–24.

Huang, G.-B., Zhu, Q.-Y., and Siew, C.-K. (2004). Extreme learning machine: A new learning scheme of feedforward neural networks. In *Proceedings of International Joint Conference on Neural Networks (IJCNN)*.

Huang, G.-B., Zhu, Q.-Y., and Siew, C.-K. (2006a). Extreme learning machine: Theory and applications. *Neurocomputing*, 70:489–501.

Huang, G.-B., Zhu, Q.-Y., and Siew, C.-K. (2006b). Real-time learning capability of neural networks. *IEEE Transaction on Neural Networks*, 17(4):251255.

Kabsch, W. and Sander, C. (1983). Dictionary of protein secondary structure: pattern recognition of hydrogen-bonded and geometrical features. *Biopolymers*, 22(12):2577–2637.

Lin, H.-H. and Tseng, L.-Y. (2010). Dbcp: a web server for disulfide bonding connectivity pattern prediction without the prior knowledge of the bonding state of cysteines. *Nucleic Acids Research*, 38:503–507.

Liu, H.-L. (2007). Recent advances in disulfide connectivity predictions. *Bioinformatics*, 2:31–47.

Lu, C.-H., Chen, Y.-C., Yu, C.-S., and Hwang, J.-K. (2007). Predicting disulfide connectivity patterns. *Proteins*, 67:262–270.

Martelli, P. L., Fariselli, P., Malaguti, L., and Casadio, R. (2002). Prediction of the disulfide bonding state of cysteines in proteins with hidden neural networks. *Protein Engineering*, 15(12):951–953.

Mucchielli-Giorgi, M., Hazout, S., and Tuffery, P. (2002). Predicting the disulfide bonding state of cysteines using protein descriptors. *Proteins*, 46:243–249.

Muskal, S., Holbrook, S., and Kim, S. (1990). Prediction of the disulfide-bonding state of cysteine in proteins. *Protein Engineering*, 3(8):667–672.

Nguyen, D. and Widrow, B. (1990). Improving the learning speed of 2-layer neural networks by choosing initial values of the adaptive weights. In *Proceedings of the International Joint Conference on Neural Networks*, volume 3, pages 21–26.

Oliphant, T. E. (2006). Guide to numpy.

Pavelka, A. and Procházka, A. (2004). Algorithms for initialization of neural network weights. *In Sborník príspevku 12. rocníku konference MATLAB*, 2:453–459.

Rubinstein, R. and Fiser, A. (2008). Predicting disulfide bond connectivity in proteins by correlated mutations analysis. *Bioinformatics*, 24(4):489–504.

Serre, D. (2002). *Matrices: Theory and applications*. Springer-Verlag New York, Inc.

Shi, O., Cai, C., Yang, H., and Yang, J. (2008). Disulfide bond prediction using neural network and secondary structure information. *The 2nd International Conference on Bioinformatics and Biomedical Engineering (ICBBE)*.

Song, J.-N., Yuan, Z., Tan, H., Huber, T., and Burrage, K. (2007). Predicting disulfide connectivity from protein sequence using multiple sequence feature vectors and secondary structure. *Bioinformatics*, 23(23):3147–3154.

Tamura, S. and Tateishi, M. (1997). Capabilities of a four-layered feedforward neural network: Four layers versus three. *IEEE Transaction on Neural Networks*, 8(2):251255.

Van Rossum, G. et al. (1991). Python language website http://www.python.org/.

Vincent, M., Passerini, A., Labbé, M., and Frasconi, P. (2008). A simplified approach to disulfide connectivity prediction from protein sequences. *BMC Bioinformatics*, 9(20).

Vullo, A. and Frasconi, P. (2004). Disulfide connectivity prediction using recursive neural networks and evolutionary information. *Bioinformatics*, 20:653–659.

Zhao, E., Liu, H.-L., Tsai, C.-H., Tsai, H.-K., Chan, C.-H., and Kao, C.-Y. (2005). Cysteine separations profiles on protein sequences infer disulfide connectivity. *Bioinformatics*, 21(8):1415–1420.

Zhu, L., Yang, J., Song, J.-N., Chou, K.-C., and Shen, H.-B. (2010). Improving the accuracy of predicting disulfide connectivity by feature selection. *Journal of Computing Chemistry*, 00(00).